Asymptotic solutions of stationary patterns in convection-reaction-diffusion systems

Olga Nekhamkina and Moshe Sheintuch
Department of Chemical Engineering, Technion-IIT, Haifa 32000, Israel
(Received 12 May 2003; published 18 September 2003)

We study and map the possible stationary patterns that emerge in a convection-reaction-diffusion (CRD) system using a learning polynomial kinetics. We classify the patterns according to the kinetic model (oscillatory, bistable, or intermediate), the instability nature of the bounded system (convective or absolute), the applied boundary conditions and the system length. This analysis presents a unifying approach to various pattern-inducing mechanisms such as DIFICI (differential flow induced chemical instability), which predicts moving patterns in systems with wide difference of convective rates, and differential capacity patterns, which predicts stationary patterns in cross-flow reactors with a large heat capacity. Previous studies of CRD systems have considered only oscillatory kinetics. Nonlinear analysis, which follows the front motion by approximating its velocity, accounts for the stability of the stationary, whether spatially periodic or other, patterns. The most dominant state is the large-amplitude stationary spatially periodic pattern. With oscillatory kinetics these emerge in the convectively unstable domain above the amplification threshold. The domain of absolute instability, which is determined analytically for unbounded systems, is divided in the bounded system into two subdomains with moving DIFICI waves or stationary patterns. With bistable kinetics the large-amplitude stationary patterns can be sustained only within a narrow subdomain but other stationary patterns, that incorporate several fronts upstream and an ''almost homogeneous'' tail downstream, can be sustained as well. With intermediate kinetics the large-amplitude axisymmetric stationary patterns may coexist with small-amplitude stationary nonaxisymmetric patterns.

DOI: 10.1103/PhysRevE.68.036207 PACS number(s): 05.45.−a, 82.40.Bj, 82.40.Ck

I. INTRODUCTION

The search for chemical mechanisms that induce stationary patterns has been a subject of intensive investigation for the past three decades. Most mechanisms employ an activator-inhibitor (Y-X) interaction with a sufficiently wide difference of their diffusive, convective, or capacity properties. The appropriated two-variable one-dimensional model may be written in the following general form:

$$\mathrm{Le}Y_t + V_1 Y_z - D_1 Y_{zz} = f(Y,X),$$

$$X_t + V_2 X_z - D_2 X_{zz} = g(Y,X), \qquad (1)$$

subject to boundary conditions at the inlet ($z=0$) and outlet ($z=L$). The seminal work by Turing [1] showed that patterns may emerge in reaction-diffusion systems (i.e., with $V_i=0$) when $f(Y,X)$ is autocatalytic and the inhibitor diffusivity D_2 is sufficiently larger than D_1.

Pattern formation in convection-reaction-diffusion (CRD) systems has been a subject of intensive investigation for past ten years. In a series of works Rovinsky and co-workers [2,3] showed that this class can generate *moving patterns* when the activator convection rate is sufficiently small when compared with that of the inhibitor ($V_1 \ll V_2$ with $\mathrm{Le}=1$ or $V_1=V_2$ with $\mathrm{Le}\gg 1$ [3]) and termed this mechanism as differential flow induced chemical instability (DIFICI). The DIFICI patterns emerge in the convectively unstable media (to be explained below) and, contrary to the Turing case, the ratio of diffusion coefficients is not essential for this mechanism. Shvartsman and Sheintuch [4] simulated moving patterns for system (1) with $V_1=0, D_2=0$, and $\mathrm{Le}\gg 1$. Both Turing and DIFICI instabilities arise from spatial decoupling of the activator and the inhibitor due to differential transport either by diffusion or convection, respectively.

Stationary pattern formation mechanism in CRD systems has been suggested by Kuznetsov *et al.* [5] for a case of equal convection rates and equal capacities, but different diffusivities, using a Brusselator kinetic model in a domain of parameters where the corresponding lumped system admits an oscillatory behavior. The authors have demonstrated that stationary patterns emerge in the convectively unstable domain as the system response to the permanent perturbations introduced by the boundary conditions, which differ from the steady state solutions. Almost simultaneously we have proposed the same idea for a CRD system when the activator capacity is sufficiently large ($\mathrm{Le}\gg 1$), while both the inhibitor and activator flow at the same rate [6–10]; the inhibitor diffusivity is not crucial for the establishment of these patterns and it can be set to zero. We suggest to name this phenomenon as the differential capacity pattern (DCP).

The CRD models described above can be grouped into two main categories. In the first one the authors (Refs. [11–13] following Ref. [5]) considered a case of equal convective velocities and capacities in a domain of parameters that admits an oscillatory behavior in the corresponding lumped system ($Y_t=f, X_t=g, \mathrm{Le}=1$); pattern selection depends then on whether the system is absolutely or convectively unstable, while the type of bifurcations (sub-critical or supercritical) depends on the kinetic model. In the second group the authors considered a system with either different convective velocities [14,15] or with different capacities of the components [6–8]. The employed methodology involved the construction of neutral curves which bound the domain of stable homogeneous solutions. Note that for a first group the neutral curve cannot be constructed using the velocity as a bi-

furcation parameter [see remark after Eq. (17) below]. In the studies of the second group the effect of transition from absolute to convective instability has not been considered yet.

The source of differences between the various models stems from different interests. The motivation for our studies is the analysis of catalytic reactors, which are characterized by a large heat capacity, by an immobile phase and by one or two fluid phases. In previous works we employed a cross-flow reactor model with a first-order Arrhenius kinetics, which is generic to studies of commercial reactors [16]. In such kinetic models the lumped system may admit multiple steady state or oscillatory solutions with a variety of phase-plane dynamics including simple oscillations around one or several steady states and complex oscillations in the case of two consecutive reactions [17]. The related distributed CRD systems may exhibit a rich plethora of patterns including stationary spatially multiperiodic patterns or spatiotemporal regular or even chaotic patterns [9,10]. We have shown that the emerging stationary spatial patterns in the limit of large V can be classified according to that of the related lumped mixed system. The variety of the system behaviors hinders a comprehensive analysis that elucidates the essential features of the model.

The purpose of this work is to derive asymptotic solutions of CRD systems using linear and nonlinear analysis in order to present a comprehensive analysis of possible patterns. To that end, and in order to derive analytical results, we use here a learning polynomial kinetics that admits oscillatory as well as multiple solutions. Note that previous studies employed oscillatory kinetics only using the Brusselator model or Gray-Scott kinetics [5,11–15]. We have constructed neutral stability curves for each of the homogeneous steady state solutions of the corresponding unbounded system. To analyze the pattern selection the absolute instability thresholds are derived both for the unbounded and for the bounded systems. Our results show that bistable kinetics, which is a common feature to many (especially exothermic and activated) reactions, may introduce a rich plethora of patterned solutions.

The structure of this work is as follows: in the following section the mathematical model and its asymptotes are formulated, linear analysis and bifurcation diagrams for an unbounded system are presented in Sec. III. Nonlinear analysis based on the examination of the front motion is conducted in Sec. IV, and in Sec. V numerical simulation of a bounded system are compared with analytical predictions.

II. MATHEMATICAL MODEL AND ITS ASYMPTOTES

In this section we will consider a two-variable one-dimensional model that describes the spatiotemporal system behavior and which will be referred to as the full partial differential equation (PDE) version of the system. Two relevant ordinary differential equations (ODE) asymptotes can be easily derived from it: the first describes the temporal behavior of the corresponding mixed system, i.e., lumped with respect to the space coordinate, while the second describes the steady state solutions of the distributed system.

We consider a full model with a learning polynomial kinetics:

$$\mathrm{Le}\frac{\partial Y}{\partial t}+V\frac{\partial Y}{\partial z}-\frac{\partial^2 Y}{\partial z^2}=f(Y,X)=-Y^3+Y+X,$$

$$\frac{\partial X}{\partial t}+V\frac{\partial X}{\partial z}=g(Y,X)=\gamma(X_w-X)-\beta Y, \tag{2}$$

subject to the Danckwerts' boundary conditions

$$Y_z(0)=V[Y(0)-Y_{in}],\quad Y_z(L)=0,\quad X_z(0)=X_{in}. \tag{3}$$

Note that the diffusion term is neglected in the second equation, so that the "pure" Turing mechanism is "*a priori*" eliminated. A similar model, but with $f(Y,X)=B\mathrm{Da}(1-X)\,h(Y)-\gamma_y(Y-Y_w)$, $g(Y,X)=\mathrm{Da}(1-X)h(Y)-\gamma_x(X-X_w)$, $h(Y)=\exp[\epsilon Y/(\epsilon+Y)]$, where $\mathrm{Da}, B, \gamma_x, \gamma_y$, and ϵ are constants, was employed in our studies of DCP [6–8] and it describes a cross-flow reactor where the feed is evenly dispersed along the reactor. The commonality of behaviors between the cubic polynomial kinetics and the generic Arrhenius kinetics was demonstrated in a variety of reactor systems such as the plug-flow reactor [18] or a catalytic system with global coupling [19]. The Danckwerts' boundary conditions are common in models of chemical reactors, and allow the system to converge to one of two common reactor asymptotes (a continuous stirred tank reactor, CSTR, or a plug flow reactor, PFR). In order to simplify the following analysis (to reduce the types of a possible system behavior) we set $X_w=0$.

The solutions of the right-hand side of Eqs. (2) $[f(Y_s,X_s)=g(Y_s,X_s)=0]$ are the asymptotic homogeneous solutions of the problem. For $\gamma=0$ only a single steady state $(Y_{s0}=X_{s0}=0)$ exists. For $\gamma\neq 0$ with $\beta<\gamma$ system (2) possesses two additional steady states: $Y_{s\pm}=\pm\sqrt{(1-\alpha}, X_{s\pm}=-\alpha Y_{s\pm}$, where $\alpha=\beta/\gamma$.

The lumped model. We begin our analysis by determining the behavior of the corresponding mixed system

$$\mathrm{Le}\frac{dY}{dt}=f(X,Y),\quad \frac{dX}{dt}=g(X,Y). \tag{4}$$

The Jacobian matrix of the linearized equations evaluated at a steady state is

$$\mathbf{J}=\begin{pmatrix}(-3Y_s^2+1) & 1\\ -\beta & -\gamma\end{pmatrix}. \tag{5}$$

The corresponding phase planes defined by the null curves $f(X,Y)=g(X,Y)=0$ exhibit an *oscillatory* [Fig. 1(a)], a *bistable* [Fig. 1(b)], or an *intermediate* [Fig. 1(c)] behavior. A standard linear stability analysis shows that the null trivial state $(Y_{s0}=X_{s0}=0)$ is stable in a range $1/\mathrm{Le}\gamma<1<\alpha$. The two other steady states $(Y_{s\pm},X_{s\pm})$ are stable if $\alpha<\min\{\frac{2}{3}+\mathrm{Le}\gamma/3,1\}$. Note that increasing Le stabilizes the system; in the notation of catalytic reactors Le is the ratio of solid to fluid heat capacities (Lewis number).

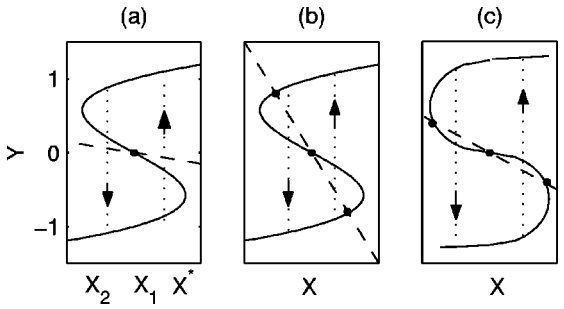

FIG. 1. Typical phase planes showing the $f(Y,X)=0$ (solid line) and $g(Y,X)=0$ (dashed lines) null curves for the cases of oscillatory (a), bistable (b), and intermediate kinetics (c). X_i mark the X values at the ith front position, X^* is the limit value. Dotted lines with arrows show the oscillatory cycles. Dots mark the steady state solutions.

Stationary solutions in an unbounded system. To understand the stationary patterns admitted by an unbounded system (2) let us consider the corresponding system that describes the stationary spatially distributed solutions (i.e., $\partial Y/\partial t=\partial X/\partial t=0$)

$$\frac{dX}{dz}=\frac{1}{V}g(X,Y), \quad \frac{dY}{dz}=p, \quad \frac{dp}{dz}=-f(X,Y)+Vp. \quad (6)$$

Linear stability analysis applied to Eq. (6) reveals that a bifurcation to a spatially periodic solutions occurs at $V=V_0$ with a spatial wave number $k=k_0$:

$$k_0^2=\mathrm{Tr}, \quad V_0^2=-j_{22}+\frac{\Delta}{k_0^2}, \quad (7)$$

where j_{ik}, Tr and Δ are the elements, trace, and determinant of the Jacobian matrix (5). Thus, the critical parameters for the null steady state are

$$k_{00}^2=1-\gamma, \quad V_{00}^2=\frac{\gamma(\alpha-\gamma)}{k_{00}^2}. \quad (8)$$

The necessary condition for the bifurcation to exist is

$$\gamma<\min\{\alpha,1\}.$$

For the other steady states the critical parameters are

$$k_{0\pm}^2=k_{00}^2-3(1-\alpha), \quad V_{0\pm}^2=\gamma+\frac{2\gamma(1-\alpha)}{k_{0\pm}^2} \quad (9)$$

and the necessary condition for the bifurcation to exist is

$$\frac{2+\gamma}{3}<\alpha<1.$$

The (spatially) oscillatory branches, that bifurcate from the homogeneous solutions at points V_0, were traced numerically by means of the continuation and bifurcation code AUTO [20] (Fig. 2).

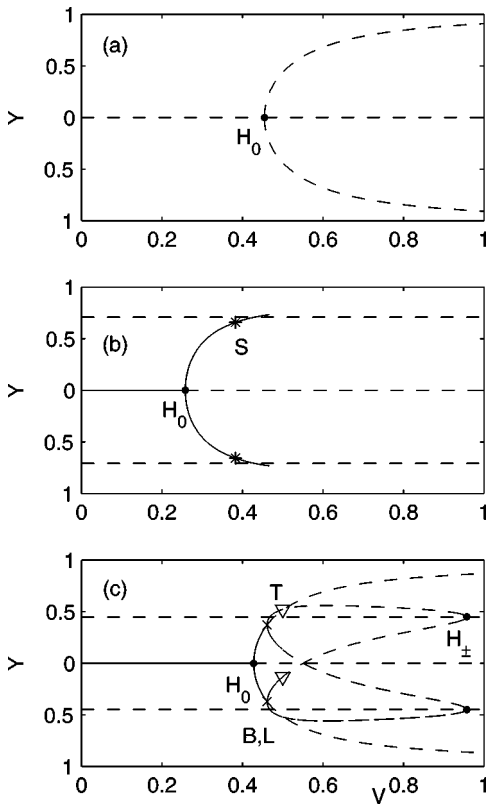

FIG. 2. Typical bifurcation diagrams of stationary solutions of ODE system (6) for an oscillatory [(a), $\alpha=1.2$], bistable [(b), $\alpha=0.5$], and intermediate kinetics [(c), $\alpha=0.8$]. Solid and dashed lines denote stable and unstable solutions, respectively. Points denote the Hopf bifurcation of the null (H_0) and upper/lower ($H_\pm$) steady states, stars in (b) denote the loss of stability S, crosses in (c) are branch points which coincide with the loop points B,L, and triangles in (c)—the Torus bifurcation T. (Le$=100,\beta=0.2$).

The bifurcation diagrams discussed below will be used as a guide for the possible steady states of the full PDE system (2) but their stability will change. Thus, the stability features described below are specified for the form of Eqs. (6) and denote stability with varying z. We refer to a bifurcation to a spatially oscillating solution as a Hopf bifurcation, even when it may occur from an unstable state.

For an *oscillatory* kinetics ($\alpha>1$) only a single (null) unstable steady state exists, and it admits a single supercritical Hopf bifurcation at $V=V_{00}$ [H_0, Fig. 2(a)].

For a *bistable* kinetics ($\alpha<\frac{2}{3}$) the bifurcation diagram is composed of two branches of unstable upper and lower steady states and a stable branch of the intermediate solution which undergoes a supercritical Hopf bifurcation at $V=V_{00}$ [point H_0 in Fig. 2(b)]. This oscillatory branch looses stability at a certain point S as it approaches the upper/lower steady states (we did not trace this branch further).

In the *intermediate* domain ($\frac{2}{3}<\alpha<1$) the unstable upper/lower steady states undergo subcritical Hopf bifurcations at $V=V_{0\pm}$ [point $H_\pm$, Fig. 2(c)]. The emanating branches of asymmetric oscillations are unstable until the Torus bifurcation [points denoted by T at the upper oscillatory branch, Fig. 2(c)] and become stable until the loop point

L, where they merge. The stable branch of the null solution, as in the previous case, undergoes a supercritical Hopf bifurcation. The emanating branch of axisymmetric stable oscillatory solutions crosses the oscillatory branches that are born from the upper/lower steady states at a branch point B which coincides with the loop point [L, Fig. 2(c)]. All oscillatory branches undergo period-doubling bifurcations, but we did not trace these branches.

III. LINEAR STABILITY ANALYSIS OF THE UNBOUNDED SYSTEM

We will start with a linear analysis of unbounded system (2) in an infinitely long region. Denoting the deviation from the basic steady state solution $\mathbf{U_s}=\{X_s, Y_s\}$ as $\mathbf{u}=\{x,y\}$, we obtain the following linearized equations:

$$\mathrm{Le}\frac{\partial y}{\partial t}+V\frac{\partial y}{\partial z}-\frac{\partial^2 y}{\partial z^2}=j_{11}y+j_{12}x,$$

$$\frac{\partial x}{\partial t}+V\frac{\partial x}{\partial z}=j_{21}y+j_{22}x. \tag{10}$$

We suppose that the initial conditions are

$$y|_{t=0}=f_0(z), \quad x|_{t=0}=g_0(z), \tag{11}$$

where the functions $f_0(z)$ and $g_0(z)$ decay rapidly for $z\to\infty$. We will search a solution of Eq. (10) in the form of the normal modes

$$\mathbf{u}(t,z)=\mathbf{u}_0 e^{\sigma t+ikz}. \tag{12}$$

Following the standard approach, we can perform a Laplace transform of system (10) with respect to the two variables z and t. The corresponding forward and backward transforms are

$$\mathbf{w}_{\sigma,k}(\sigma,k)=\int_0^\infty e^{-\sigma t}dt\int_{-\infty}^{\infty}\mathbf{u}(t,z)e^{-ikz}dz \tag{13}$$

and

$$\mathbf{u}(t,z)=-\frac{1}{4\pi^2}\int_{-i\infty+s_0}^{i\infty+s_0}e^{\sigma t}d\sigma\int_{-\infty}^{\infty}\mathbf{w}_{\sigma,k}e^{ikz}dk, \quad s_0=\mathrm{Re}\sigma_0. \tag{14}$$

Here we assume that the perturbations grow not faster than $\exp(s_0 t)$, so that the integral in the right-hand side of Eq. (13) converges, and in Eq. (14) the integration contour in the σ plane (parallel to the imaginary axis) is located to the right of all singularities of the integrand. The integration contour in the k plane should be the imaginary axis. The components $w_{\sigma,k}$ can be found from the transformed system (10) in the following form:

$$\mathbf{w}_{\sigma,k}=\frac{\mathbf{h}(\sigma,k)}{\mathcal{D}(\sigma,k)}. \tag{15}$$

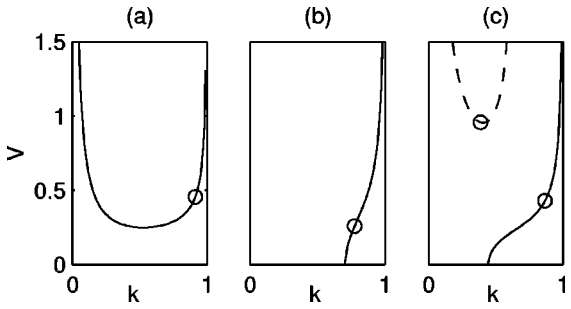

FIG. 3. Typical neutral curves for the null (solid line) and the upper/lower steady states (dashed line). Open circles denote the amplification threshold of stationary patterns [Eqs. (8) and (9)]. Cases (a)–(c) and the corresponding parameters as in Fig. 2.

Here the denominator is a characteristic function which defines a dispersion relation of the system, while the numerator depends both on the system parameters and the initial perturbations (their Laplace transforms). To that end we assumed that the denominator has no singularities as a function of complex variables σ,k.

Nontrivial solutions exist with a set of (σ,k) obeying the dispersion relation $\mathcal{D}(\sigma,k)=0$:

$$\mathrm{Le}\sigma^2+\sigma[k^2-j_{11}-\mathrm{Le}j_{22}+iVk(\mathrm{Le}+1)]+\Delta-k^2(V^2+j_{22}) +iVk(k^2-\mathrm{Tr})=0. \tag{16}$$

The bifurcation condition for instability $\mathrm{Re}\sigma=0$ with real spatial wave numbers ($\mathrm{Im}k=0$) obeys the following relation:

$$Q^2(j_{22}k^2-\Delta)+j_{22}k^2V^2(\mathrm{Le}-1)^2(k^2-j_{11})=0,$$

$$Q=k^2-j_{11}-\mathrm{Le}j_{22}. \tag{17}$$

Note that with $\mathrm{Le}=1$ the onset of instability does not depend on the flow rate.

Neutral curves. For a case $\mathrm{Le}\neq 1$ we can construct neutral curves using the velocity V as a bifurcation parameter:

$$V^2=\frac{Q^2(j_{22}k^2-\Delta)}{-j_{22}(\mathrm{Le}-1)^2(k^2-j_{11})k^2}. \tag{18}$$

The stability analysis of the homogeneous solution of the distributed system with $V\to 0$ agrees, of course, with the corresponding results of the lumped model [Eqs. (4)] discussed above.

For the null steady state and $\alpha>1$ the neutral curve acquires a minimum [at V_m, k_m; Fig. 3(a)] and traveling waves can be excited only with $V>V_m$. When $\alpha<1$ the neutral curve is a monotonically increasing curve emanating at the critical point $k_T=\Delta/j_{22}=\sqrt{(}1-\alpha$ [Figs. 3(b),(c)]. For all $V>0$ the homogeneous state is unstable and can exhibit traveling waves with a finite k.

The two other steady states $X_{s\pm}$ are stable for all V in a domain $0<\alpha<2/3$. The neutral curve can be constructed in a domain $2/3<\alpha<1$ and it acquires a minimum in similarity to the case of the null steady state with $\alpha>1$ [Fig. 3(c)].

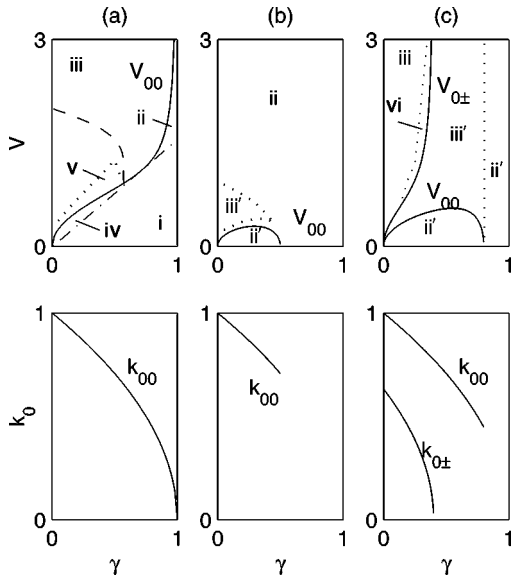

FIG. 4. Typical bifurcation diagrams in the (V,γ) plane (upper row) mapped by the following lines: The stationary pattern threshold of the null and upper/lower states ($V_{00}, V_{0\pm}$, solid lines). The locus of minima of the neutral curve [V_m, dashed-dotted line in (a)]. The absolute instability thresholds for an unbounded [V_a, dashed line in (a)] and bounded [V_a^b, dotted line in (a)] system. Dotted lines in (b) and (c) denote the boundaries of the oscillatory domains: V_{00}^l and V_{00}^u in (b) and $V_{0\pm}^u$ in (c). The boundaries marked by dotted lines in (a)–(c) were computed numerically. The lower row presents the critical wave numbers of the stationary pattern for the null and upper/lower states ($k_{00}, k_{0\pm}$). Large-amplitude spatially periodic patterns exist in domain (iii) or (iii′), moving patterns in (iv), small-amplitude patterns in (vi), see text for other behaviors. (Parameters Le, α as in Fig. 2).

The amplification threshold of stationary perturbations. The condition for stationary patterns to emerge is

$$\sigma = 0, \quad \mathrm{Im}k = 0. \tag{19}$$

Applying these conditions to the dispersion relation (16) we obtain the critical parameters V_0, k_0, corresponding to the amplification threshold of stationary perturbations. It obviously coincides with the Hopf bifurcation point of the lumped system (6), i.e., it is defined by Eq. (7). The corresponding critical points are marked on the neutral curves by circles (Fig. 3). The critical parameters as functions of kinetic parameters are shown in Fig. 4. For the null steady state the bifurcation point exists in a range $\gamma < \min(1,\alpha)$. For the other steady states the amplification threshold exists in a domain $(2+\gamma)/3 < \alpha < 1$. Note that the wave number of the null solution k_{00} is larger, while the critical velocity is smaller than the corresponding values of the lower/upper steady states $(k_{0\pm}, V_{0\pm})$.

The type of instability. Now we have to determine whether the instability is absolute or convective. An instability is *convective* if a small perturbation propagates forward as a wave packet growing in size, but at any given location the disturbance from the steady state decays with time as $t \to \infty$ [21,22]. In contrast, the instability is *absolute* if the initial perturbation grows unbounded in time, at any fixed point in the laboratory frame. The effect of permanent perturbations that are applied at the boundary of a bounded system is closely related with the type of instability of the corresponding unbounded system (see discussion at the end of this section).

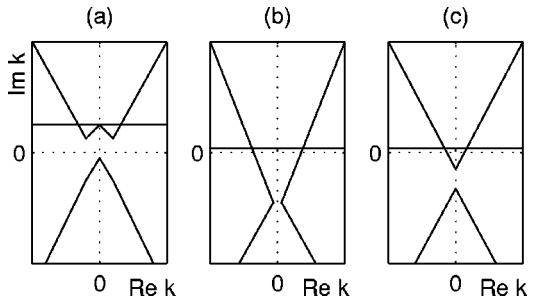

FIG. 5. Schematic diagrams showing the k-roots behavior of the dispersion relation (16) with critical $\mathrm{Re}\sigma = 0$ for a case of a stable (a), absolutely unstable (b), and convectively unstable (c) system.

In order to analyze the type of instability of the unbounded system (2) it is necessary to study the asymptotic behavior of the solution $u(t,z)$ defined by Eq. (14) at $t \to \infty$. We will follow an approach proposed in Ref. [21]. If for a certain V each of the complex k-roots of the dispersion relation $\mathcal{D}(\sigma,k,V) = 0$ with $\mathrm{Re}\sigma = 0$ and varying $\mathrm{Im}\sigma$ belongs to either the upper or lower complex k half planes, then the system is stable [Fig. 5(a)]. If one of the k-roots crosses the real axis, then the system is unstable (we can find a root of dispersion relation with $\mathrm{Re}\sigma = 0$ and $\mathrm{Re}k \neq 0$). Note that in an unstable system the perturbations are spatially amplified ($\mathrm{Im}k$ of at least one of the k roots changes the sign).

The instability is convective if we can construct the k contour for the inner integral in Eq. (14) that will round the singularities of the integrand $\mathbf{w}_{\sigma,k}$ defined by Eq. (13) [Fig. 5(b)]. Such manipulation is possible if the k contour is not pinched between two poles that approach the contour from opposite sides and merge [Fig. 5(c)]. So the critical case implies the existence of a double root of the dispersion relation [or a branch point $k = k_b(\sigma_b)$] that satisfies

$$\mathcal{D}(\sigma_b, k_b) = 0, \quad \frac{d\sigma_b}{dk_b} = 0. \tag{20}$$

The critical velocity V_a, corresponding to $\mathrm{Re}\sigma_b = 0$, defines a transition from the convective to absolute instability. System (20) was solved numerically. The calculated values of V_a are shown in Fig. 4(c) (dashed lines).

The analysis presented above was conducted for an unbounded system. It may be applied for a bounded system if the reflection of exciting waves from the boundaries may be neglected (i.e., for time intervals that are smaller than the time propagation of the a signal along the system). In general, the spectrum of wave numbers in a bounded system is finite and is defined by boundary conditions. However, for sufficiently long systems the dispersion relation depends on intrinsic properties of the system itself and does not depend on the applied BC (boundary conditions) [23]. The stability of a bounded system reflects the stability of the correspond-

ing unbounded system as follows [23]: If the unbounded system is absolutely unstable, the bounded one will be globally unstable, while if the unbounded system is convectively unstable the bounded one can be either unstable, or stable. Thus, in the bounded system with V above the amplification threshold of stationary perturbations [Eq. (7)], the patterns will be stationary if the unbounded system is convectively unstable, while if the unbounded system is absolutely unstable, one can expect to find complex patterns composed of an upstream zone with several stationary waves and moving waves in the downstream zone.

IV. PHASE-PLANE ANALYSIS AND FRONT MOTION

To complement the linear analysis above and the study of possible steady solutions (Fig. 2) we present below an analysis that follows the fronts in Y and their dependence on the interaction with X profile, capitalizing on the slow front motion and the fast X adjustment. The analysis is valid for wide separation of fronts, implying $\gamma \ll 1$.

We start with the analysis of front in Y for fixed X (say $X=X_0$). That is possible in the domain where $F(Y,X_0)$ is bistable and we can find two pseudohomogeneous solutions away from the inlet and a front solution that separates the two stable steady states. Imagine the flow directed to the right and an ascending front separating low-Y downstream (left) from high-Y upstream. The front position Z_f is described by ($\tau = t/\mathrm{Le}$)

$$dZ_f/d\tau = -C(Z_f,X_0) = -C_{\infty,V=0}(X_0) - (C_{V=0} - C_{\infty,V=0}) + V, \quad (21)$$

where a positive front velocity C implies an expansion of the high-Y domain. (In the general case we should allow for the dependence of C on X and on parameters). The expression incorporates three terms: the first is the front velocity in an unbounded system with no convection ($C_{\infty,V=0}$) and the other two show corrections that we have introduced for this velocity (Ref. [18]): The effect of convection is to push the front at the fluid velocity. The other effect, due to boundary conditions [the second term in Eq. (21)] decays exponentially with the distance and is ignored for now. For fixed $X=X_0$, the front velocity $C_{\infty,V=0}(X_0)$ is monotonically changing with X_0 or any other parameter; for a cubic polynomial function $F(Y,X_0) = -Y^3 + Y + X_0$ and with small X_0 it is $C_{\infty,V=0}(X_0) \simeq 3X_0/\sqrt{2}$. Thus, $C_{\infty,V=0}=0$ only for a certain set of parameters and typically we do not expect to find stable stationary fronts with or without convection. The stationary front, which exists if $C_{\infty,V=0}=V$, is simply a boundary between fronts that propagate upstream or downstream.

We turn now to study the effect of varying X. To simplify the analysis assume that X is responding fast ($\mathrm{Le} \gg 1$) and its balance is assumed to be in steady state. Its solution then is

$$X = X(0)e^{-\gamma z/V} + X_w(1-e^{-\gamma z/V}) - \frac{\beta}{V}e^{-\gamma z/V}\int_0^z e^{\gamma z^*/V} Y dz^*, \quad (22)$$

and the system is described by

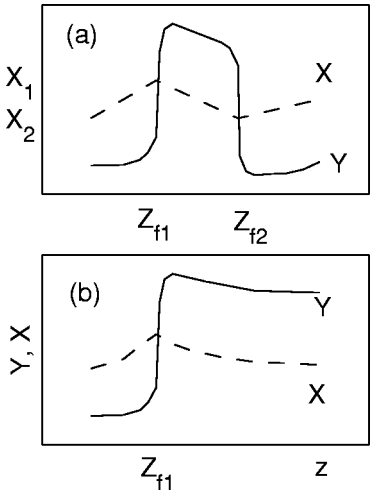

FIG. 6. Schematic profiles of the state variables $Y(z)$ and $X(z)$ for a stable spatially patterned state (a), corresponds to phase planes shown in Figs. 1(a),(b), and a single front pattern (b).

$$Y_\tau + VY_z - Y_{zz} = -Y^3 + Y + X(Y) = \tilde{F}(Y). \quad (23)$$

To analyze the system we distinguish between several cases: The effect of convection is expressed in the flow rate V and the effect of kinetics should be classified according to the possible homogeneous steady solution that is established away from the feed [$\tilde{F}(Y_s)=0$].

Oscillatory kinetics with $\gamma = 0$. To simplify analysis even further set $\gamma = 0$ so that $X(z) = X(0) - (\beta/V)\int_0^z Y dz^*$. This is a typical behavior within the oscillatory domain. Now consider a family of fronts with positions at $Z_{f1}, Z_{f2}, \ldots$ and the corresponding X values of $X_1, X_2, \ldots$ [Fig. 6(a)]; the first front and the other odd ones are assumed to be ascending, i.e., separate a low-Y domain on the left from a high-Y domain on the right, while the others (even) are descending fronts. Their positions, ignoring the interaction between the fronts and interaction with the boundaries, are described by

$$dZ_{f1}/d\tau = -C(X(Z_{f1})) + V,$$

$$X(Z_{f1}) = X_1 = X_0 - \frac{\beta}{V}\int_0^{Z_{f1}} Y dz^*, \quad (24a)$$

$$dZ_{f2}/d\tau = -C(X(Z_{f2})) + V,$$

$$X(Z_{f2}) = X_2 = X_1 - \frac{\beta}{V}\int_{Z_{f1}}^{Z_{f2}} Y dz^*. \quad (24b)$$

Since for the first front $Y<0$ on the left domain, X increases with z and the position of the first front is stable: perturbation of the front position to the left encounters lower X, which encourage expansion of the cold (low-Y) domain, while perturbation to the right encounters an opposite behavior (recall that X responds instantaneously). The stability can be verified mathematically by examining dC/dZ_{f1}. Small changes in V will induce small changes in the front position. A similar analysis applies to the next front, showing that it is stable over a wide domain of V's.

To a first approximation, ignoring the effect of gradient in X on C, the fronts are stationary when

$$C(X_i)=V,$$

which allows us to calculate analytically X_i values at the front positions [Fig. 1(a) marks X_1, X_2 and Fig. 6(a)—the corresponding Z_{fi}]. For an ascending and descending fronts we find $X_{i+1}=-X_i$ for this symmetric cubic kinetics. For small V, as C is linear with X ($C=\kappa X_0$), the stationary front position varies like $Z_{f1}\sim V^2-\kappa V X_0$. (As $V\to 0$ the front interaction with the boundary cannot be ignored and the pattern will collapse; note that the bifurcation to a pattern solution $V_{00}\to 0$ as $\gamma\to 0$). For larger V, however, the front velocity that corresponds to X value at the limit point [X^*, Fig. 1(a)] will be exceeded; yet even under these conditions the stationary front is sustained but now it moves as a phase front rather than a trigger front (see Ref. [24] for the distinction between trigger and phase fronts).

Thus, under certain conditions, and with $\mathrm{Le}\gg 1$, system (2) sustain stationary-periodic patterns. For $X(0)=0$ the problem is symmetric and the wavelength ($Z_{f2}-Z_{f1}=2Z_{f1}$) could be computed analytically.

Oscillatory kinetics with $0<\gamma\ll 1$ *and* $X_0=0$. The approximate analysis can be extended also for $\gamma>0$ and it will be useful to analyze the pattern on the (Y,X) plane [Fig. 1(a)]: The section upstream from the front is described by Eqs. (22) and (23) and the profile of X is ascending (although not linearly); within the oscillatory domain, when the null state ($Y_s=X_s=0$) is the only homogeneous state, the front (first) will become stationary at a certain position where $C(X(Z_{f1}))=V$, and we follow the same procedure as earlier in determining Z_{f1} etc. Again $Z_{f2}-Z_{f1}=2Z_{f1}$ is the wavelength and we will find periodic stationary solutions for all V exceeding a critical value.

Within the bistable domain [Fig. 1(b)] we always find two stable homogeneous solutions with no fronts where the system, far from the entrance, asymptotically reaches one of these homogeneous steady solutions [Fig. 6(b)], depending on the inlet Y value. Aside from these we can find other solutions that incorporate fronts. The behavior should be classified into two situations.

(a) At low V, when the X value that sustain a stationary front does not exceed the steady state value [$X_1(V)<X_s$, Fig. 1(b)] we can find stationary periodic solutions, identical to those described above [see Fig. 6(a)]. With proper initial conditions, however, we can also find solutions that incorporate one, two, or several fronts upstream and a homogeneous solution downstream [see simulated patterns in Fig. 8(a), to be discussed below]. Note that these conditions imply adjacent fronts and we have ignored front interaction.

(b) At large V, when $X_1(V)>X_s$, such fronts are washed out of the reactor and the system approaches the asymptotically homogeneous state: To argue that point consider the front in Fig. 6(b); the behavior upstream from the front is qualitatively similar to that described above in Fig. 6(a), but the X profile does not attain the stationary condition $X=X_1$. Consequently, the front propagates upstream and exits the system. This analysis explains the domain of stationary fronts at low γ and low V [Fig. 3(a)].

Excitable kinetics with $\gamma>0$ *and* $X_0\neq 0$. A similar analysis can be applied in this case, where the phase plane corresponds to an excitable system. We will not pursue it here.

V. NUMERICAL SIMULATIONS

We want to show now how the transition from a homogeneous solution to stationary patterns with increasing V is affected by the type of instability (absolute or convective), by the BC and by the reactor length. To that end we plot bifurcation maps in the (V,γ) plane for a set of parameters that corresponds to oscillatory, bistable, or intermediate kinetics. A typical bifurcation map was constructed by drawing the following analytically computed lines: $V=V_m(\gamma)$—the locus of minima of the neutral curve, $V_{00}(\gamma)$ and $V_{0\pm}(\gamma)$—the stationary pattern threshold for the null and upper/lower states, respectively. Also drawn were several numerically computed lines such as $V_a(\gamma)$ and $V_a^b(\gamma)$—the absolute instability thresholds for an unbounded and bounded system, respectively.

We choose $\mathrm{Le}=100$ and set the reactor length to $L=100$ in most of simulations in order to resolve the structure of the emerging patterns; several runs (marked in the text) were conducted with $L=200$.

Numerical simulations of the full PDE system (2) were carried out by means of an implicit finite difference scheme based on the method of fractional steps [25].

Oscillatory kinetics ($\alpha>1$). In this case the unbounded system (2) possesses a single homogeneous (null) steady state, which is stable in a domain of low flow rates and undergoes a supercritical bifurcation to moving waves with increasing V.

The stationary patterns threshold V_{00} is tangent to V_m at $\gamma\simeq 0.7$; the corresponding wave number k_{00} coincides with $k_m(\gamma)$, it exceeds k_m in the domain $\gamma<0.7$ [Fig. 3(a)] and is smaller than $k_m(\gamma)$ in the domain $\gamma>0.7$. The absolute instability threshold of an unbounded system (V_a) exists in a domain of small γ and is terminated at the intersection point with the $V_m(\gamma)$ line. For a bounded system the numerically determined V_a^b line varies with L and with increasing L it tends to the asymptotic value V_a of unbounded system [system (20)]. These lines divide the (V,γ) plane (Fig. 4) to the following domains and solutions (the same notation is employed below and in Fig. 4):

(i) The homogeneous solution is established below $V_m(\gamma)$ and moving wave cannot be excited; if $Y_{in}\neq 0$ or $X_{in}\neq 0$ then the solution exhibits some adjustment at the inlet section due to the boundary conditions.

(ii) Pseudo homogeneous patterns are established for $V_m<V<V_0$ and outside the absolute instability domain; it is similar to domain (i), but transient moving waves can be excited, before being gradually washed out of the system. Note that numerically obtained critical velocities V_0 practically coincide with analytical predictions for the unbounded system (8).

(iii) Stationary patterns [similar to Fig. 7(c)] are established for most of the domain with $V>\max[V_0,V_a^b]$. The cal-

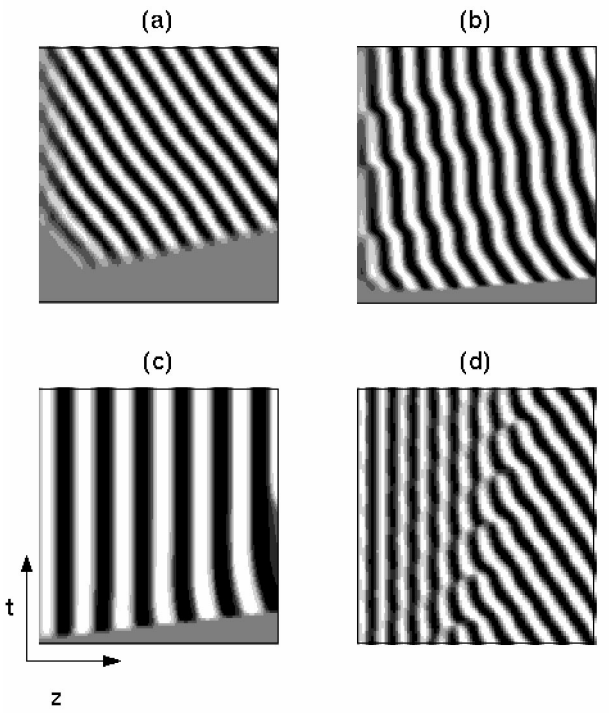

FIG. 7. Typical solutions presented as a spatiotemporal gray-scale pattern of Y for the case of the oscillatory kinetics: (a) moving waves [domain (iv) in Fig. 4(a)], (b) zigzag pattern [imposed by small perturbations of BC, domain (v) in Fig. 4]; also formed in domain (v) are (c) stationary patterns (large perturbation of BC), and (d) transient patterns (in response to a change of BC). $\alpha = 1.2, \beta = 0.36$; $V = 0.65$ (a), 0.85 (b–d). In (d) the coordinates (t,z) are rescaled for convenience.

culated spatial amplitudes and the periods of oscillations are in a very good agreement with the corresponding values obtained by means of the continuation approach [20]. Note that for large V the dispersion term becomes insignificant with respect to convective transport, and the period of spatial oscillation varies linearly with V. (The space coordinate can be rescaled as z/V and the dispersion term in the transformed coordinate is multiplied by $1/V^2$).

(iv) Propagating waves with a narrow "boundary layer" near the inlet [Fig. 7(a)] are excited for $V_m < V < V_0 < V_a^b$ (i.e., within the absolute instability domain). These waves are exactly the self-sustained DIFICI patterns. For relatively small deviations $V - V_m$ the calculated wave velocity C_w and the spatial wave number k are in a good agreement with analytical predictions for the unbounded system, using the parameters at the minimum of the neutral curve ($k \simeq k_m, C_w = \omega_m / k_m$).

(v) For $V_0 < V < V_a^b$ the system behavior is highly sensitive to the applied BC showing either moving or stationary waves: For small deviations of the boundary values (X_{in} or Y_{in}) from the null steady state the system exhibits moving waves, which can be significantly affected (modulated) by BC forming a zigzag structure [Fig. 7(b)]. With relatively large (yet, fixed) perturbations at the boundaries the system exhibits stationary patterns composed of spatially periodic waves over most of the reactor [Fig. 7(c)]; the applied BC affect only the length of the boundary layer. With appropriate choice of initial conditions we can induce complicated patterns composed of two zones with slightly oscillating quasi-stationary patterns in the upstream zone and moving waves in the downstream zone [Fig. 7(d)]. The boundary between the wave packets is drifting and over a long time one of them (depending on the BC) suppresses the other.

With time-dependent BC it is possible to transform the sustained stationary patterns into moving ones and vice versa (let during a certain time interval we impose X_{in} or Y_{in} that slightly deviate from X_s, Y_s, then the system will exhibit zigzag patterns; if in the following time interval we will choose X_{in} or Y_{in} that differ significantly from X_s, Y_s, then the patterns will be transformed into stationary ones [Fig. 7(d)]. Moreover, with appropriate stepwise changes in BC it is possible to generate complicated patterns composed of alternating stationary, oscillatory, and moving wave zones propagating in opposite directions.

With increasing L (or varying α) we expect to find a subdomain adjusted to the lower boundary $[V_0(\gamma)]$ for which stationary patterns cannot be sustained at all, independent of the BC. However such simulations are very time consuming and are out of the scope of the present study.

Bistable kinetics ($\alpha < 2/3$). In this case the unbounded system (2) possesses three homogeneous steady states: the upper and lower are stable everywhere and are globally stable for most of the domain, while the null solution is unstable for all $V \geqslant 0$. The only other stable state is a stationary pattern which exists for a bounded system between the lower [V_{00}^l, close to V_{00}, a lower dotted line in Fig. 4(b)] and the upper boundaries [V_{00}^u, an upper dotted line in Fig. 4(b), corresponds to state S in Fig. 2(b)]; these boundaries were calculated by direct simulations. Note that while the null steady state is absolutely unstable in the unbounded system (for $V < V_{a0}$), the bounded system is convectively unstable only due to the existence of the other stable solutions. These form the following domains [Fig. 4(b)] which are marked in similarity to those of the previous case:

(ii′) For $V < V_{00}^l$ and $V > V_{00}^u$ the system attains one of the pseudohomogeneous steady states. Axisymmetric waves can be excited during a transient process, but they are washed out upstream with small V, γ and downstream for large V, γ.

(iii′) Stationary patterns with spatially periodic or other structures can be sustained for $V_{00}^l < V < V_{00}^u$. With appropriate choice of the initial conditions it is possible to design patterns composed of several stationary fronts in the upstream section and one of the stable steady state in the downstream zone [Fig. 8(a)]; these were discussed in the preceding section.

In a relatively narrow sub-domain [$V_{00} < V < V_{00}^l$, not marked in Fig. 4(b)] the system attains a pseudohomogeneous state, similarly to domain ii, but during a transient process the excited moving waves are transformed into spatially oscillatory patterns which, in turn, are eventually terminated [Fig. 8(b)]. Probably the wave length becomes too small to counteract the interaction between the nearest fronts.

Intermediate kinetics ($2/3 < \alpha < 1$). This case is the most complex among those considered and we found two kinds of

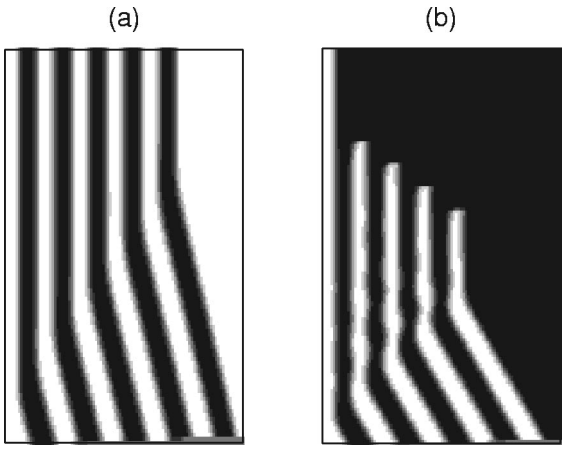

FIG. 8. Typical spatiotemporal solutions presented as a gray-scale pattern of Y for the bistable kinetics case showing (a) regular stationary patterns [domain (iii′) in Fig. 4(b)] and (b) transient process in a subdomain below it leading to a gradual termination of stationary waves. $\alpha=0.5,\beta=0.2$; $V=0.4$ (a), 0.375 (b).

spatially periodic solutions (axisymmetric or not) as well as the pseudohomogeneous solutions. Of the three steady states the null solution, as in the previous case, is unstable for all $V>0$, while the upper/lower solutions loose stability via a Hopf bifurcation and become convectively unstable at $V>V_{m\pm}$. The thresholds of stationary patterns exist in a domain $\gamma<\alpha$ for the null steady state and in a domain $\gamma<3\alpha-2$ for the upper/lower solutions with $V_{00}<V_{0\pm}$ [Fig. 4(c)].

As in the previous case we found domain (ii′), where the system admits a pseudohomogeneous solution and can exhibit transient waves of axisymmetric amplitudes. Stable spatial pattern states are sustained with $V>V_{00}$. In domain (iii′) ($V_{00}<V<V_{0\pm}$) complex "designer" patterns, composed of several stationary fronts upstream and a homogeneous steady state downstream can be sustained. They coexist with stable pseudohomogeneous solutions. In domain (iii) (above region vi, see below) stationary spatially periodic patterns are the only stable solutions of the system. Note that contrary to the case of bistable kinetics, domains (iii) and (iii′) have no upper boundaries with increasing V.

The more intricate system behavior takes place in a relatively narrow domain (vi) above the amplification threshold of nonaxisymmetric patterns $V_{0\pm}$. Just above $V_{0\pm}$ with $V<V^{u}_{0\pm}$ [dotted line in Fig. 4(c)] the system exhibits stationary spatially periodic patterns with small-amplitude oscillations around the corresponding steady states [Fig. 9(a)]. With increasing V the spatial periodicity is lost and the amplitude of the oscillations becomes space dependent [grows downstream, Fig. 9(b)]. With the following increasing V the pattern selection becomes sensitive to the reactor length L: For moderate L ($\leqslant 100$ with $\gamma=0.167,\alpha=0.8$) and with increasing V, the zone of small-amplitude spatial oscillations is shifted downstream and for very large V we obtained pseudohomogeneous solution, defined by the applied BC. With increasing L the stationary patterns of varying spatial amplitude around upper/lower steady state become unstable and switch in the downstream zone into moving waves with

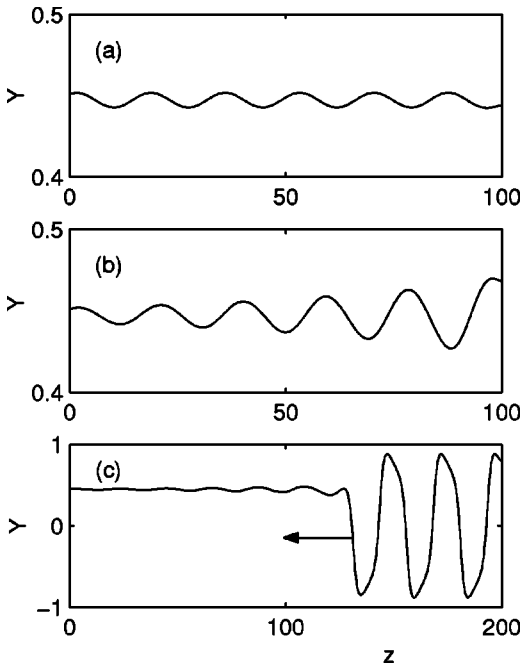

FIG. 9. Typical solutions for the case of the intermediate kinetics in the domain of coexistence of different types of stationary patterns [(vi), Fig. 4(c)] showing (a) a small-amplitude nonaxisymmetric stationary pattern, (b) a similar profile with an increasing downstream-amplitude, and (c) a transient process leading to formation of large-amplitude axisymmetric patterns. $\alpha=0.8,\beta=0.2$; $V=1$ (a), 1.1 (b,c); $L=100$ (a,b), 200 (c).

large-amplitude axisymmetric spatial oscillations. These waves propagate upstream and conquer the whole spatial domain forming eventually stationary spatially periodic patterns of the same type as when the null steady state is used as the initial condition [the profile shown in Fig. 9(c) illustrates the transition process: large amplitude waves at the downstream zone propagate upstream].

VI. CONCLUDING REMARKS

The mechanism of stationary patterns formation in the CRD (convection-reaction-diffusion) system with large separation of time scales ($\mathrm{Le}\gg 1$) is analyzed for a learning cubic kinetics. The study revealed that pattern selection depends on kinetic model (the type of the phase plane of the corresponding mixed model), the type of instability, the applied boundary conditions, and the reactor length.

For *oscillatory* kinetics stationary spatially periodic patterns emerge in the *convectively* unstable domain above the amplification threshold $V=V_{00}$. The domain of *absolute* instability is divided, in the bounded system, into two subdomains: one with moving DIFICI waves and another with stationary patterns. The boundary between the two varies with the boundary conditions imposed and the system size.

For *bistable* kinetics the stationary patterns with spatial oscillations around an intermediate steady state can be sustained within its convectively instability domain in a bounded region far from the basins of attraction of the homogeneous stable states. Other stationary patterns, that in-

corporate several fronts upstream and an ''almost homogeneous'' tail downstream [Fig. 8(a)], can be sustained as well.

For *intermediate* kinetics (the upper/lower steady states admit a Hopf bifurcation) the stationary patterns with spatial oscillations around the upper/lower steady states can be sustained in a narrow domain above the amplification threshold $V=V_{0\pm}$. These patterns coexist with stationary large-amplitude axisymmetric patterns.

Numerical simulations results confirm analytical predictions by linear stability analysis. Nonlinear analysis, which follows the front motion by approximating its velocity, accounts for the stability of the stationary, whether spatially periodic or other, patterns.

The results presented above were obtained with a learning kinetics for a range of parameters when the corresponding lumped system exhibits oscillatory or bistable kinetics. Previous studies of CRD systems [5,11–15]. have considered only oscillatory kinetics. In our previous works [6–8] we considered a cross-flow reactor model with a first-order Arrhenius kinetics. In such a kinetic model the lumped system may admit multiple steady states or oscillatory solutions with a variety of phase-plane dynamics including simple oscillations around one or several steady states and complex oscillations in the case of two consecutive reactions [9,10]. We considered there a case that may admit multiple homogeneous solutions and have shown that the CRD system behavior can be very complex, but in the limit of $\mathrm{Pe}_i = LV_i/D_i \to \infty$ the emerging stationary spatial patterns can be classified according to that of the related lumped mixed system ($Y_z=f, X_z=g$). That work motivated the present study, in which the simpler kinetics employed allowed for systematic analysis and the derivation of some analytical results.

ACKNOWLEDGMENTS

This work was supported by the US-Binational Scientific Foundation. M.S. is a member of the Minerva Center of Nonlinear Dynamics. O.N. was partially supported by the Center for Absorption in Science, Ministry of Immigrant Absorption State of Israel.

[1] A.M. Turing, Philos. Trans. R. Soc. London, Ser. A **237**, 37 (1952).
[2] A.B. Rovinsky and M. Menzinger, Phys. Rev. Lett. **69**, 1193 (1992).
[3] V.Z. Yakhnin, A.B. Rovinsky, and M. Menzinger, Chem. Eng. Sci. **49**, 3257 (1994).
[4] M. Sheintuch and S. Shvartsman, Chem. Eng. Sci. **49**, 5315 (1994).
[5] S.P. Kuznetsov, E. Mosekilde, G. Dewel, and P. Borckmans, J. Chem. Phys. **106**, 7609 (1997).
[6] O.A. Nekhamkina, A. A Nepomnyashchy, B.Y. Rubinstein, and M. Sheintuch, Phys. Rev. E **61**, 2436 (2000).
[7] O.A. Nekhamkina, B.Y. Rubinstein, and M. Sheintuch, AIChE J. **46**, 1632 (2000).
[8] O.A. Nekhamkina, B.Y. Rubinstein, and M. Sheintuch, Chem. Eng. Sci. **56**, 771 (2001).
[9] O.A. Nekhamkina and M. Sheintuch, Phys. Rev. E **66**, 016204 (2002).
[10] M. Sheintuch and O. Nekhamkina, AIChE J. **49**, 1241 (2003).
[11] P. Andresén, M. Bache, E. Mosekilde, G. Dewel, and P. Borckmanns, Phys. Rev. E **60**, 297 (1999).
[12] J.R. Bamforth, S. Kalliadasis, J.H. Merkin, and S.K. Scott, Phys. Chem. Chem. Phys. **2**, 4013 (2000).
[13] J.R. Bamforth, J.H. Merkin, S.K. Scott, R. Tóth, and V. Gáspár, Phys. Chem. Chem. Phys. **3**, 1435 (2001).
[14] R.A. Satnoianu and M. Menzinger, Phys. Rev. E **62**, 113 (2000).
[15] R.A. Satnoianu, P.K. Maini and M. Menzinger, Physica D **160**, 79 (2001).
[16] K.R. Westerterp, W.P.M. Van Swaaij, and A.A.C.M. Beenackers, *Chemical Reactor Design and Operation* (Wiley, New York, 1984).
[17] D.V. Jorgensen and R. Aris, Chem. Eng. Sci. **38**, 45 (1983).
[18] M. Sheintuch, Y. Smagina, and O. Nekhamkina, Ind. Eng. Chem. Res. **41**, 2136 (2002).
[19] U. Middya, D. Luss, and M. Sheintuch, J. Chem. Phys. **101**, 4688 (1994).
[20] E.J. Doedel, Congr. Numer. **30**, 265 (1981).
[21] R.J. Briggs, *Electro-Stream Interaction with Plasmas* (MIT Press, Cambridge, MA, 1964).
[22] R.J. Deissler, J. Stat. Phys. **40**, 371 (1985).
[23] E.M. Lifshits and L.P. Pitaevskii, *Physical Kinetics* (Pergamon, Oxford, 1981).
[24] A.S. Mikhailov, *Foundation of Synergetics I. Distributed Active Systems* (Springer-Verlag, Berlin, 1990).
[25] N.N. Yanenko, *The Method of Fractional Steps; the Solution of Problems of Mathematical Physics in Several Variables* (Springer, Berlin, 1971).